Fin ray patterns at the fin-to-limb transition

Thomas A. Stewart[a,1], Justin B. Lemberg[a], Natalia K. Taft[b], Ihna Yoo[a], Edward B. Daeschler[c], and Neil H. Shubin[a,1]

[a]Department of Organismal Biology and Anatomy, University of Chicago, Chicago, IL 60637; [b]Department of Biological Sciences, University of Wisconsin–Parkside, Kenosha, WI 53141; and [c]Department of Vertebrate Zoology, Academy of Natural Sciences of Drexel University, Philadelphia, PA 19103

Contributed by Neil H. Shubin, November 20, 2019 (sent for review September 17, 2019; reviewed by John R. Hutchinson and Adam Summers)

The fin-to-limb transition was marked by the origin of digits and the loss of dermal fin rays. Paleontological research into this transformation has focused on the evolution of the endoskeleton, with little attention paid to fin ray structure and function. To address this knowledge gap, we study the dermal rays of the pectoral fins of 3 key tetrapodomorph taxa—*Sauripterus taylori* (Rhizodontida), *Eusthenopteron foordi* (Tristichopteridae), and *Tiktaalik roseae* (Elpistostegalia)—using computed tomography. These data show several trends in the lineage leading to digited forms, including the consolidation of fin rays (e.g., reduced segmentation and branching), reduction of the fin web, and unexpectedly, the evolution of asymmetry between dorsal and ventral hemitrichia. In *Eusthenopteron*, dorsal rays cover the preaxial endoskeleton slightly more than ventral rays. In *Tiktaalik*, dorsal rays fully cover the third and fourth mesomeres, while ventral rays are restricted distal to these elements, suggesting the presence of ventralized musculature at the fin tip analogous to a fleshy "palm." Asymmetry is also observed in cross-sectional areas of dorsal and ventral rays. *Eusthenopteron* dorsal rays are slightly larger than ventral rays; by contrast, *Tiktaalik* dorsal rays can be several times larger than ventral rays, and degree of asymmetry appears to be greater at larger sizes. Analysis of extant osteichthyans suggests that cross-sectional asymmetry in the dermal rays of paired fins is plesiomorphic to crown group osteichthyans. The evolution of dermal rays in crownward stem tetrapods reflects adaptation for a fin-supported elevated posture and resistance to substrate-based loading prior to the origin of digits.

dermal skeleton | evolution | fin-to-limb transition | paleontology

The fin-to-limb transition is characterized by the loss of fin rays (dermal skeletal rods that support the fin web) and the evolutionary origin of digits (1–3). Traditionally, efforts to explain how limbs evolved from fins have focused on transformation and novelty in the endoskeleton (4–18), with little emphasis placed on fin ray structure and function. Detailed anatomical description of dermal rays is lacking, in part, due to taphonomic bias. Individual rays are small, positioned superficially on the fin, and likely to be displaced during preservation. Additionally, when fossils are prepared, it is common practice for the dermal skeleton to be removed to allow for visualization of the endoskeleton beneath (19–21). This deficit in our knowledge is unfortunate: given the functional (22) and developmental (23, 24) integration of these skeletal systems in fins, comparative analyses of the dermal skeleton of tetrapodomorph paired fins can help elucidate how one of the greatest transitions in vertebrate history occurred.

General features of tetrapodomorph paired fins include an endoskeleton that is overlapped significantly by dermal rays that are tightly packed (i.e., with little fin membrane between them) and covered proximally by scales (25–27). The fins can be divided into a lobed region, which contains endoskeleton and fin musculature, and the fin web, which contains rays extending beyond the endoskeleton and interray webbing (28). The rays are ossified and diagnosed as lepidotrichia [sensu Goodrich (25)] because dorsal and ventral rays (hemitrichia) run apposed to one another for extended distances in the fin web. Rays are usually segmented, branching, and more robust on the anterior, or leading edge, of the fin (25, 26). In some tetrapodomorph clades, fin ray morphology is a diagnostic character. For example, rhizodontids have a long unsegmented proximal region that spans most of the ray's length (29, 30), and rays of the osteolepid *Gogonasus andrewsae* have distinctive perforations and cross-sectional geometry (31). Broadly, the distribution and polarity of fin ray characters within tetrapodomorphs are undescribed, although it is hypothesized that fin rays were reduced and ultimately lost as fin function shifted from resisting hydrodynamic forces to substrate-based loading (32).

To understand how dermal rays evolved in the paired fins of tetrapodomorph fishes, we analyzed pectoral fins of 3 key taxa, which are listed here by increasing proximity to the tetrapod crown group. First, we studied the rhizodontid *Sauripterus taylori* (Hall, 1843), both juvenile (33) and adult specimens (20, 34). Second, we studied the tristichopterid *Eusthenopteron foordi* (Whiteaves, 1881), which is known from a complete postlarval growth series (35–37). Both *Eusthenopteron* and *Sauripterus* are hypothesized to have been fully aquatic and to have used their pectoral fins primarily for swimming (20, 33, 37, 38) and perhaps, also to prop the animal up while resting on benthic substrate. Third, we studied the elpistostegid *Tiktaalik roseae* (Daeschler, Shubin & Jenkins, 2006), the most crownward finned tetrapodomorph (39–41) known from at least 20 individuals that are estimated to range from 1.25 to 2.75 m in length (12, 42). Based on study of the endoskeleton and girdle, the pectoral fin of *Tiktaalik* is hypothesized to have been capable of holding the body up in an elevated posture on the substrate, and the animal is predicted to have occupied a benthic aquatic niche in littoral zones (12, 42, 43). The microcomputed

Significance

To explain how limbs evolved from fins, paleontologists have traditionally studied the endoskeleton. Here, we provide a comparative analysis of the other skeletal system of fins, the dermal skeleton. We describe dermal ray anatomy for 3 species of tetrapodomorph fishes. These data show that, prior to the origin of digits, dermal rays were simplified, the fin web became reduced in size, and the top and bottom of the fin became more asymmetric. These changes reveal how fins became adapted for interacting with the substrate prior to the fin-to-limb transition and that dorsoventral asymmetry is an important, understudied axis of diversification in paired fins.

Author contributions: T.A.S., J.B.L., N.K.T., E.B.D., and N.H.S. designed research; T.A.S., J.B.L., N.K.T., I.Y., and N.H.S. performed research; T.A.S., J.B.L., I.Y., and N.H.S. analyzed data; N.K.T., E.B.D., and N.H.S. conceived the project; and T.A.S. wrote the paper.

Reviewers: J.R.H., Royal Veterinary College; and A.S., University of Washington.

Competing interest statement: N.H.S., J.R.H., and A.S. are coauthors on a 2017 Perspective article. They have not collaborated scientifically.

Data deposition: Computed tomography data reported in this paper are available on MorphoSource (accession no. P853). Measurements of fin rays reported in this paper are available on Dryad Digital Repository (DOI: 10.5061/dryad.2fqz612kd). The R code for analysis and plotting is available on GitHub (https://github.com/ThomasAStewart/tetrapodomorph_dermal_project).

[1]To whom correspondence may be addressed. Email: tomstewart@uchicago.edu or nshubin@uchicago.edu.

This article contains supporting information online at https://www.pnas.org/lookup/suppl/doi:10.1073/pnas.1915983117/-/DCSupplemental.

First published December 30, 2019.

tomography (μCT) data presented here show several trends in the evolution of dermal rays along the tetrapod stem including, unexpectedly, the evolution of dorsoventral asymmetry.

Results

Pectoral Fin Rays of *Sauripterus*. To visualize the pectoral fin rays of *S. taylori*, the specimen ANSP20581 was μCT scanned (*SI Appendix*, Table S1). The material includes the right pectoral fin of an adult individual (*SI Appendix*, Fig. S1). Dorsal hemitrichia are preserved partially embedded in matrix. Ventral hemitrichia were manually removed from the specimen during fossil preparation, and data on their distribution and morphology are unavailable. The fin was slightly deformed during preservation. Repositioning the fin to a more natural and articulated position requires only moderate translation of endoskeletal elements (*SI Appendix*, Fig. S2 and Movie S1). Hypotheses regarding the distribution of pectoral fin rays, discussed below, are not affected by this reconstruction.

At least 60 hemitrichia are present on the dorsal surface of the pectoral fin of *Sauripterus* (Fig. 1*A*). This is consistent with the ∼65 rays observed in a cf. *Sauripterus* juvenile, ANSP20980 (Fig. 1*B*) (33), and indicates that nearly the full complement of dorsal hemitrichia is preserved. In ANSP20581, 20 rays are associated with the radius, 12 rays are distal to the intermedium, and at least 28 are distal to the ulnare (Fig. 1*A*). Dorsal rays extend proximally to fully cover the radius, cover the distal half of the intermedium, and fully cover distal radials 5 through 8. The fin rays are unsegmented and presumed to represent only the proximal portion of a large fin web, as is observed in juveniles (Fig. 1*B*) (20, 33). At their distal tips, rays can be segmented (33) and were likely branching, similar to other rhizodontids (29).

Rays vary in their morphology along the anteroposterior axis of the pectoral fin. In ANSP20581, along the anterior edge of the radius are 2 or 3 robust rays with geometry that is quite distinct from the more posterior rays. These anterior-most rays are dorsoventrally flattened and have broad bases, while the more posterior rays have tapering bases and are circular in their cross-section with a hollow core (20). Expanded anterior fin rays are also observed in the juvenile specimens (Fig. 1*B*) (33).

Pectoral Fin Rays of *Eusthenopteron*. To characterize dermal rays of the pectoral fin of *Eusthenopteron*, 2 specimens were μCT scanned (*SI Appendix*, Table S1). CMNH 8153 includes a pair of pectoral fins. The right fin is exposed in dorsal aspect, and the left fin is positioned in a similar orientation but embedded in matrix (*SI Appendix*, Fig. S3). The orientation of these fins was determined by the curvature of the proximal articular surface of the radius (27). Neither fin was preserved with a humerus, and the dermal fin skeleton is disturbed for much of the left pectoral fin. CMNH 10926 comprises 2 pieces and includes an entire fish preserved in lateral aspect with the left side exposed. The anterior piece contains the skull, trunk, and pectoral fins (*SI Appendix*, Fig. S4). Portions of both left and right pectoral fins are preserved. The right fin, which is embedded in matrix, is more complete and missing the proximal and posterior portions. Consistent with previous descriptions, pectoral fin rays have a proximal unsegmented region, which constitutes a small proportion of total fin ray length, and a distal segmented region, which is branching in rays posterior to the radius (Fig. 2 *A* and *B*) (27, 44).

The left pectoral fin of CMNH 8153 includes at least 30 rays (Fig. 2 *A* and *B*). Although the fin web appears generally undisturbed, it is difficult to diagnose which endoskeletal element the rays might have been most closely associated with. This is because the endoskeleton is slightly repositioned as compared with other *Eusthenopteron* specimens (e.g., here the radius exhibits a greater angle with respect to the ulna) (3, 27), and rays are sometimes damaged and missing from one of the sides (Fig. 2 *A* and *B*), making it challenging to diagnose the precise proximal extent of rays throughout the fin web. Additionally, the posterior flange of the ulnare is not preserved, and given that the pectoral fin of another specimen is described with ∼40 rays (27), postaxial rays are likely missing. The left pectoral fin of CMNH 8153 includes 7 rays closely associated with the radius (Fig. 2*C*). The right pectoral fin of CMNH 10926 includes 5 rays associated with the intermedium and 4 with the third radial (Fig. 2*D*). These counts are consistent with another specimen showing 8 rays associated with the radius, 5 with the intermedium, 5 with the third radial, 7 with the third mesomere, and 10 with the posterior flange of the third radial (27).

In *Eusthenopteron*, dorsal and ventral hemitrichia differ slightly in their spatial distributions. On the right radius of CMNH 8153, dorsal hemitrichia extend further proximally than ventral hemitrichia (Fig. 2*C*), and on the intermedium and third radial of the right fin of CMNH 10526, dorsal hemitrichia extend further proximally than ventral hemitrichia (Fig. 2*D*). Concordant patterns between these 2 specimens indicate that in *Eusthenopteron* preaxial fin rays on the dorsal surface covered more of the endoskeleton than ventral rays.

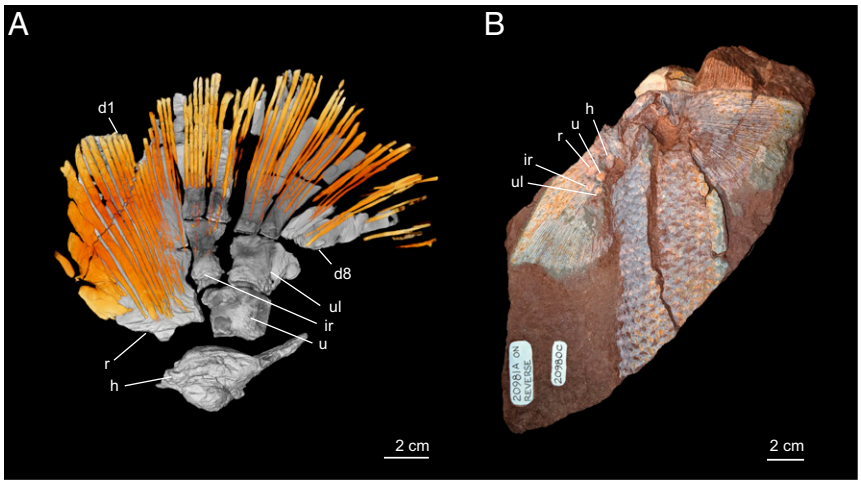

Fig. 1. Dermal rays of the pectoral fin of *S. taylori*. (*A*) Right pectoral fin of ANSP20581 in dorsal perspective. Scanning reveals several robust and flattened rays on the leading edge of the radius. Posterior rays are thinner and round in cross-section. (*B*) Photograph of ANSP20980, juvenile of cf. *Sauripterus*, showing the full extent of the fin web. d1, first distal radial; d8, eighth distal radial; h, humerus; ir, intermedium; r, radius; u, ulna; ul, ulnare.

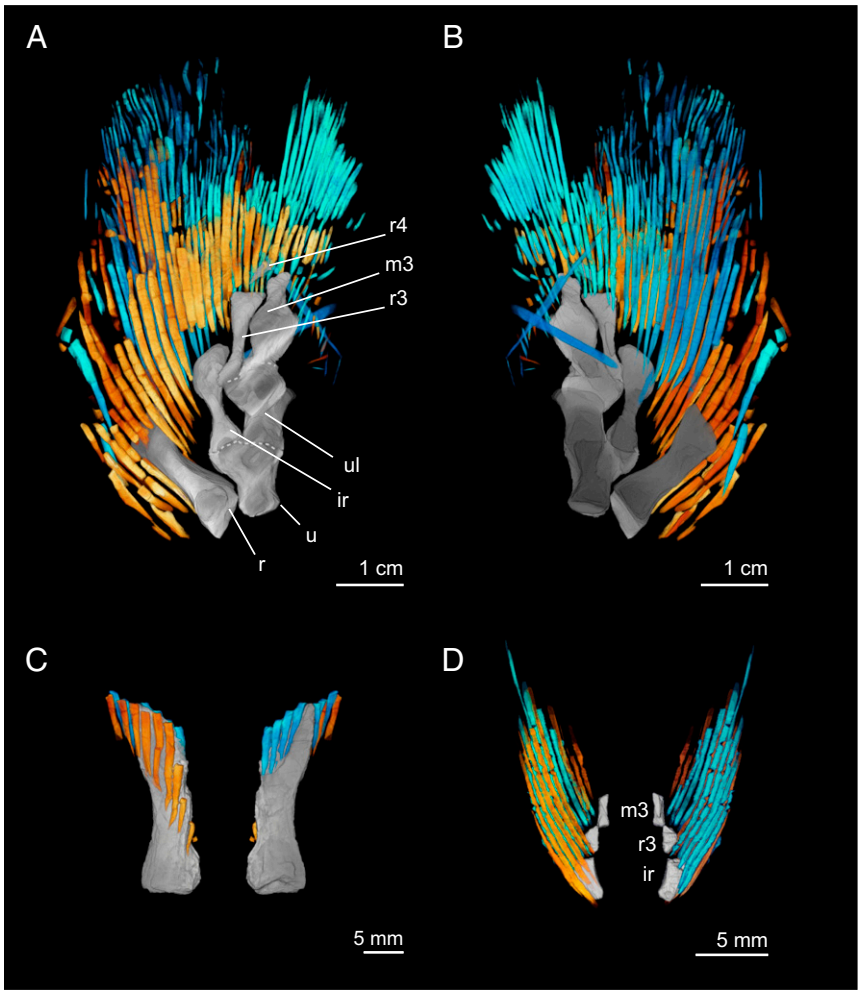

Fig. 2. Dermal rays of the pectoral fin of *E. foordi*. Left pectoral fin of CMNH 8153 in (*A*) dorsal and (*B*) ventral perspectives. (*C*) Radius of the right pectoral fin of CMNH 8153 in dorsal and ventral perspectives. (*D*) Distal and anterior portion of the right pectoral fin of CMNH 10926 in dorsal and ventral perspectives. In all images, dorsal hemitrichia are shown in yellow–orange, and ventral hemitrichia are cyan. ir, intermedium; m3, third mesomere; r, radius; r3, third radial; r4, fourth radial; u, ulna; ul, ulnare.

Pectoral Fin Rays of *Tiktaalik*. To analyze the anatomy of dermal rays of the pectoral fin of *Tiktaalik*, 3 specimens were μCT scanned (*SI Appendix*, Table S1). Pectoral fin materials are known from several *Tiktaalik* specimens; however, only 3 are preserved with dermal fin rays in close proximity with the endoskeleton. NUFV110 includes a nearly complete right pectoral fin. NUFV109 includes a mostly complete right fin with proximal elements removed so that they could be studied in isolation; the distal articulated portion was scanned. NUFV108 includes a disarticulated left pectoral fin.

In NUFV110, at least 33 lepidotrichia are preserved along the anterior and distal fin margin (Fig. 3 *A* and *B*). At least 10 rays are associated with the radius, 7 with the intermedium, 3 with each of the third and fourth radials, and 10 with the fourth mesomere. Postaxial radials and fin rays are not preserved in NUFV110. Several rays preserved on the ventral fin surface, adjacent to the ulnare, were not included in the reconstruction (Movie S2). We interpret these as having been displaced postmortem because of substantial separation between rays and the endoskeleton and because the ulnare was also preserved in a nonarticulated position. In NUFV109, 13 hemitrichia are preserved on the dorsal fin surface and 22 on the ventral fin surface (Fig. 3 *C* and *D*). These rays would have been associated with the fourth preaxial radial or fourth mesomere. It is challenging to demarcate precisely to which element they correspond due to slight anterior displacement of the rays during preservation. In NUFV108, 57 rays are preserved (*SI Appendix*, Fig. S5). Nine of these are dorsal to the radius, and the remainder is separated into 2 groups of 28 and 20 rays and not associated with particular endoskeletal elements.

The fin rays of *Tiktaalik* do not extend significantly beyond the distal terminus of the endoskeleton. Most rays are unbranching and unsegmented. In NUFV109 and NUFV110, rays sometimes exhibit fractures perpendicular to the long axis of the ray (Fig. 3 and Movies S2 and S3). However, these are diagnosed as breakage, not segmentation, on the basis of their irregular spacing and variability between rays. In NUFV109, the posterior 20 rays exhibit a characteristic distal fringe that indicates terminal segmentation and branching, which has broken apart during preservation (*SI Appendix*, Fig. S5). A similar pattern of preservation is observed in the pectoral fin of *Howittichthys*, a proposed elpistostegid (28).

Dorsal and ventral hemitrichia differ in their distribution and morphology. At the distal portion of the fin, dorsal hemitrichia overlap the endoskeleton to a greater extent than do ventral hemitrichia. In NUFV110, dorsal hemitrichia cover from the distal-most region of the fin to the proximal side of the third mesomere (Fig. 3*A*), while ventral hemitrichia are restricted terminal to fourth mesomere (Fig. 3*B*). NUFV109 shows a similar

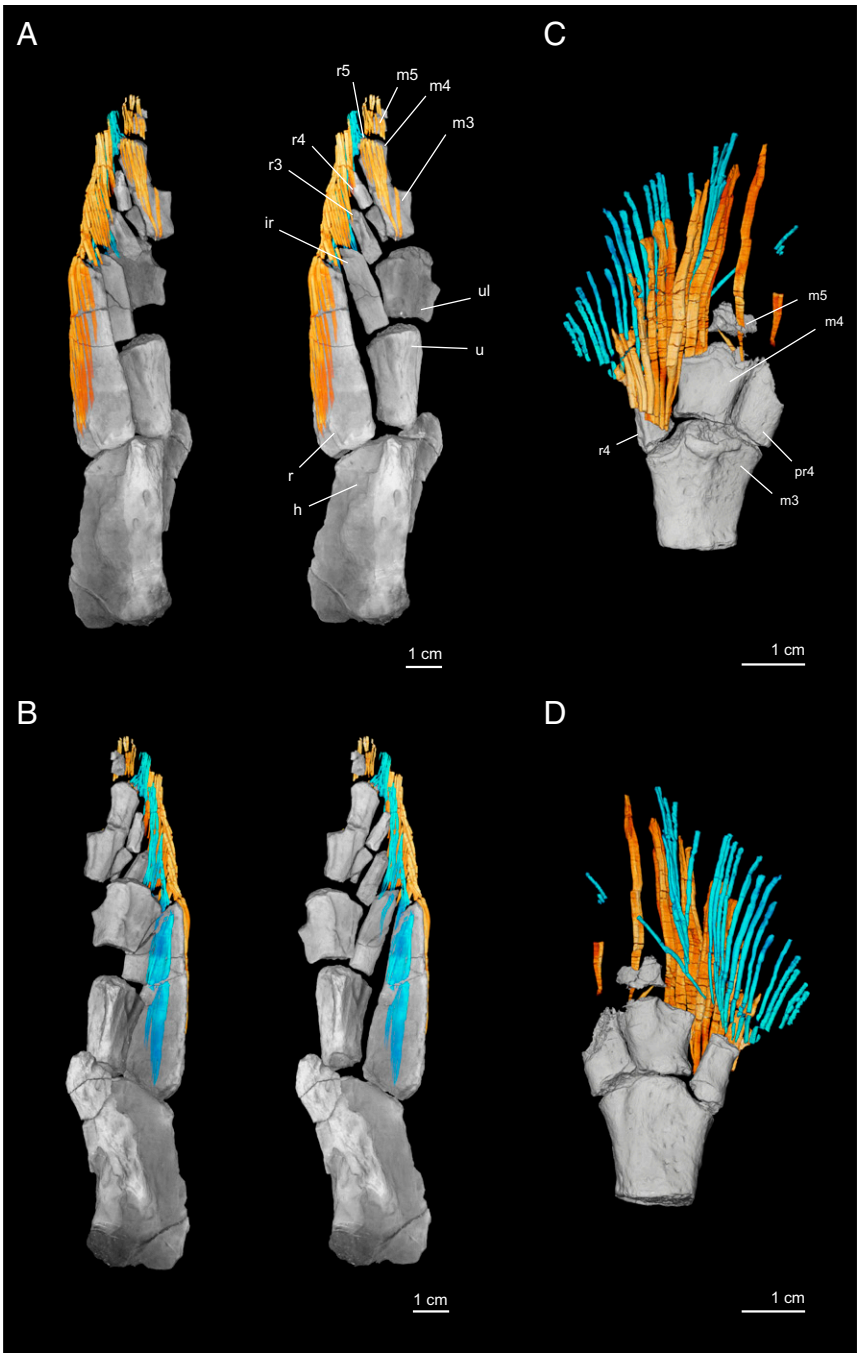

Fig. 3. Dermal rays of the pectoral fin of *T. roseae*. NUFV110 in (*A*) dorsal and (*B*) ventral perspectives. *A*, *Left* and *B*, *Left* show the specimen in the preserved position with scales and matrix removed. *A*, *Right* and *B*, *Right* show endoskeletal elements repositioned to more natural, articulated positions. NUFV109 in (*C*) dorsal and (*D*) ventral perspectives. In all images, dorsal hemitrichia are shown in yellow–orange, and ventral hemitrichia are cyan. h, humerus; ir, intermedium; m3, third mesomere; m4, fourth mesomere; m5, fifth mesomere; pr4, posterior radial adjacent to mesomere 4; r, radius; r3, radial of the third mesomere; r4, radial of the fourth mesomere; r5, radial of the fifth mesomere; u, ulna; ul, ulnare.

pattern: dorsal hemitrichia cover the fifth mesomere, the anterior edge of fourth mesomere, and its anterior radial (Fig. 3*C*), while ventral hemitrichia are positioned distal to the fourth mesomere (Fig. 3*D*). Thus, we infer that the fifth mesomere was sandwiched between a pair of hemitrichia, while the third and fourth mesomeres were covered only on the dorsal surface. Additionally, dorsal and ventral hemitrichia differ in their robustness, with dorsal hemitrichia being robust and ventral fin rays more gracile by comparison. This is most readily observed in the larger specimen, NUFV109 (Fig. 3 *C* and *D*, *SI Appendix*, Fig. S6, and Movie S3), and discussed in detail below.

Consistent patterns of asymmetry in endoskeletal coverage by hemitrichia between specimens in both *Eusthenopteron* and *Tiktaalik* suggest that the pattern is not the result of postmortem displacement of fin elements but rather, is a general feature of these fins. To test whether dorsoventral asymmetry in the coverage of fin rays relative to endoskeleton can reflect biological patterning and not simply taphonomy, we analyzed pectoral fin anatomy of

the Australian lungfish, *Neoceratordus fosteri* (Krefft 1870). Consistent with above observations of tetrapodomorphs, we observe dorsoventral asymmetry in the proximal extent of dermal fin rays. In the postaxial fin web of *Neoceratodus*, dorsal rays cover radials to a greater extent than ventral rays (Fig. 4). In other regions of the fin, the degree of coverage is similar between the dorsal and ventral rays.

μCT data also reveal details of the endoskeleton of *T. roseae*. Grooves are observed on the ventral surfaces of the ulna, ulnare, intermedium, fourth and fifth mesomeres, and radial elements anterior to these mesomeres (*SI Appendix*, 3-dimensional image). These grooves are inferred to have housed vasculature and innervation.

Comparisons of Dorsal and Ventral Hemitrichia. As noted above, the dorsal and ventral hemitrichia of *Tiktaalik* specimen NUFV109 differ dramatically from one another in their size and geometry (Fig. 3 *C* and *D*, *SI Appendix*, Fig. S6, and Movie S3). To understand how this pattern evolved and might have developed, we quantified cross-sectional area (CSA) and second moment of area (SMA) of dorsal and ventral hemitrichia in *Tiktaalik* and *Eusthenopteron*. For each taxon, we compared rays in approximately the same position within the fin web between 2 individuals of different sizes. In *Tiktaalik*, the only region of the fin where such a comparison was possible is the fin tip. In *Eusthenopteron*, we compared preaxial lepidotrichia because they are the least disturbed and most complete between the 2 specimens.

To estimate the relative sizes of *Tiktaalik* specimens, we compared humeral length, measuring from the entepicondyle to the middle of the proximal articular surface. In NUFV110, the humerus measures 5.07 cm, and in NUFV109, it measures 6.80 cm. Therefore, assuming that humeral length scales isometrically with standard length, we estimate that NUFV109 was 1.34 times the size of NUFV110. To estimate the relative sizes of the 2 *Eusthenopteron* specimens, we measured the approximate total length of CMNH 10926 (18.8 cm) and estimated the total length of CMNH 8153 by measuring the right radius (1.99 cm) and scaling this to a previous reconstruction (27). The estimated length of CMNH 8153 is 76.9 cm, near to the upper range of described specimens (35) and approximately 4 times the size of CMNH 10926.

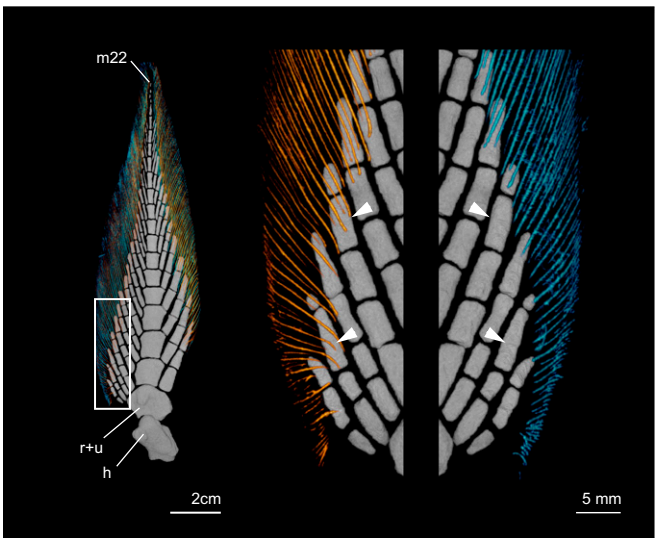

Fig. 4. Dermal rays of the pectoral fin of *N. fosteri*. Right pectoral fin showing that dorsal and ventral postaxial fin rays differ in their degree of coverage of endoskeletal elements. *Left* is the full fin in dorsal perspective. *Center* is the region of interest in dorsal perspective showing dorsal rays only. *Right* is the region of interest in ventral perspective showing ventral rays only. Dorsal hemitrichia are shown in yellow–orange, and ventral hemitrichia are cyan. Arrowheads demarcate the proximal-most extent of campotrichia on select radials. h, humerus; m22, the 22nd and distal-most mesomere; r + u, element composed of the fused radius and ulna.

For *Tiktaalik*, lepidotrichia on the preaxial side of the fourth mesomere were compared. In the smaller specimen, NUFV110, dorsal hemitrichia on average have a 1.93 times-larger CSA than the ventral rays (Fig. 5*A*). In the larger specimen, NUFV109, dorsal hemitrichia on average have a 2.67 times-larger CSA than ventral rays (Fig. 5*B*). For *Eusthenopteron*, lepidotrichia distal to the third radial were compared. Similar to *Tiktaalik*, dorsal hemitrichia have greater CSA as compared with corresponding ventral hemitrichia; however, the magnitude of asymmetry is less in *Eusthenopteron* and consistent between individuals of different sizes (Fig. 5 *C* and *D*). Dorsal rays are 1.10 and 1.09 times greater than ventral rays in CMNH 10926 and CMNH 8153, the smaller and larger specimens, respectively. All pairwise comparisons between the dorsal and ventral hemitrichia of a particular lepidotrichium show differences in CSA (Mann–Whitney *U* test, *P* value < 0.05) (*SI Appendix*, Table S2).

To assess whether dorsoventral asymmetry might be a general feature of the hemitrichia of paired fins in crown group osteichthyans, we measured the CSAs of dermal rays from the pectoral fins of *Neoceratodus* and 2 nonteleost actinopterygians, *Polypterus ornatipinnis* (Lacepède 1803) and *Acipenser brevirostrum* (Lesueur 1818), the shortnose sturgeon (*SI Appendix*, Fig. S7). In *Neoceratodus*, 6 pairs of rays were sampled across the fin web. Fin ray morphology is heterogeneous along the anteroposterior axis: anteriorly, the rays are asymmetric, with dorsal campotrichia being 1.63 times larger than ventral campotrichia; more posteriorly (pairs 4, 5), the rays are not different from one another in CSA to a threshold of $P > 0.05$, and in the most posterior pair (6), the dorsal campotrichia are 0.84 times the size of the ventral campotrichia. Pairwise comparisons between dorsal and ventral rays of campotrichia pairs 1, 2, 3, and 6 show differences in CSA (Mann–Whitney *U* test, *P* value < 0.05) (*SI Appendix*, Table S2). For *Polypterus* and *Acipenser*, rays were sampled from the middle of the fin web. In *Polypterus*, dorsal hemitrichia on average have a CSA that is 0.83 times the size of the ventral rays. In *Acipenser*, dorsal hemitrichia on average have a CSA that is 1.05 times larger than the ventral rays. All rays of *Polypterus* and *Acipenser* were analyzed, and pairwise comparisons of hemitrichia of a lepidotrichium show differences in CSA (Mann–Whitney *U* test, *P* value < 0.05) (*SI Appendix*, Table S2).

Comparisons of dorsal and ventral hemitrichia were also conducted using the SMA, a descriptor of resistance to bending. We compared the bending for each hemitrichia with a neutral axis that corresponds with the dorsoventral axis of the fin (*SI Appendix*, Fig. S8). Broadly, these results are consistent with those presented above for CSA (*SI Appendix*, Fig. S8 and Table S2). Asymmetry in SMA is greater in *Tiktaalik* than *Eusthenopteron*. In *Tiktaalik*, asymmetry in SMA is greater in the larger specimen, whereas in *Eusthenopteron*, asymmetry in SMA is consistent between sizes. These results are robust to possible alternative orientations of the ventral hemitrichia in *Tiktaalik*. Furthermore, *Polypterus* and *Acipenser* also show asymmetry in SMA, suggesting that dorsoventral asymmetries in morphology and mechanics characterize the lepidotrichia of crown group ostichthyans and that the sign and magnitude of such asymmetries differ between lineages.

Discussion

Tetrapodomorph pectoral fins vary in a number of fin ray properties, including branching, segmentation, length, and surprisingly, dorsoventral asymmetry. We analyze this variation in a phylogenetic context, taking into account what is known of the functional morphology of benthic actinopterygians and evolution of the pectoral fin endoskeleton. We argue that pectoral fins of crownward tetrapodomorphs were adapted to substrate-based

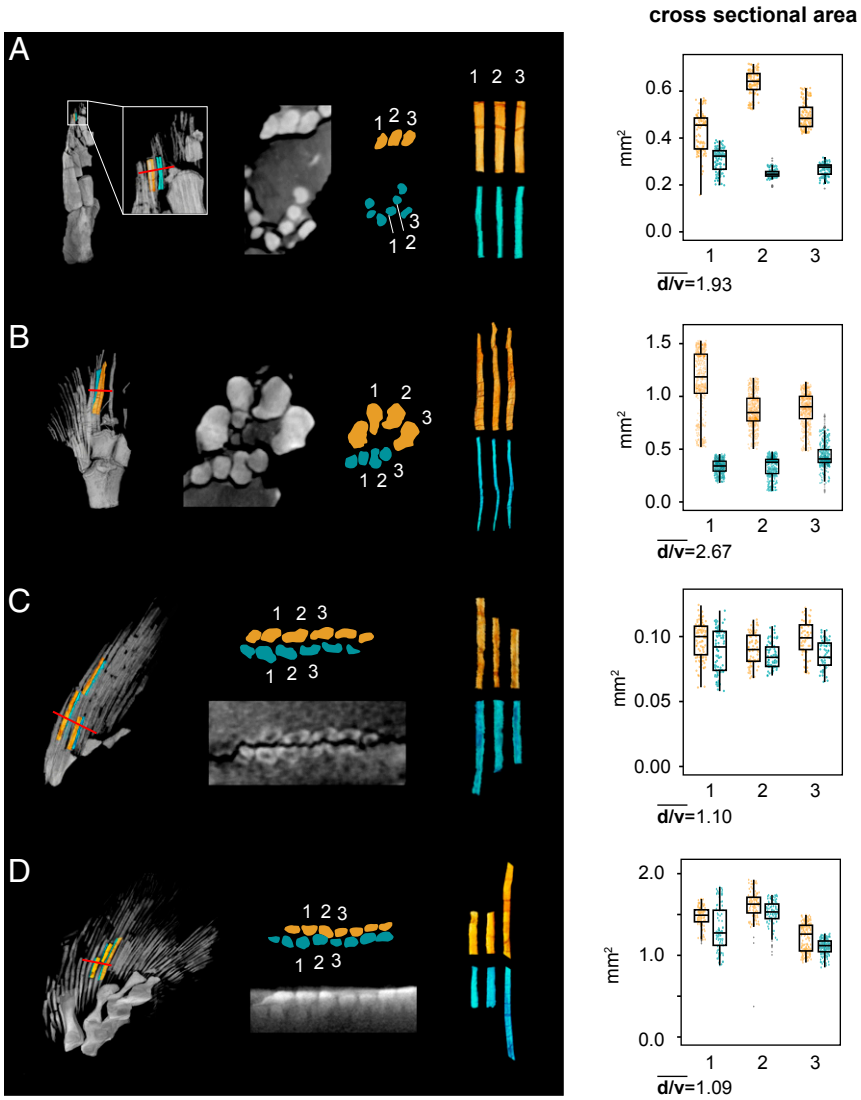

Fig. 5. Comparisons of dorsal and ventral hemitrichia *Tiktaalik* and *Eusthenopteron*. CSA was calculated for 3 pairs of hemitrichia in the pectoral fins of *Tiktaalik* and *Eusthenopteron*. In all fins, the rays that were analyzed are numbered 1 through 3 from anterior to posterior. Volumetric renderings of the fin in *Left* indicate the position of the rays that were measured and also, the position of the cross-section (denoted by red lines) figured to *Right*. For both volumetric renderings and box plots, the color orange–yellow designates dorsal hemitrichia, and the color cyan designates ventral hemitrichia. *T. roseae* is shown in (*A*) NUFV110 and (*B*) NUFV109. *E. foordi* is shown in (*C*) CMNH 10926 and (*D*) CMNH 8153. The mean ratios of dorsal to ventral hemitrichial CSAs for the 3 lepidotrichia of each fin are reported as the variable "d/v." Box plots show median value, the first and third quartiles, and maximum and minimum values; outlying points are denoted as gray dots.

loading prior to the origin of digits, that the evolution of dorsoventral patterning is an important axis of morphological diversification in paired fins, and that analyses of fin function in Tetrapodomorpha should consider both dermal and endoskeletal systems.

Convergence with Benthic Actinopterygians. In tetrapodomorph pectoral fins, rays extend further proximally on the preaxial side than on the postaxial side. *Sauripterus* and *Eusthenopteron* have rays that contact the base of the radius on the fin's leading edge and are terminal to the ulnare at the fin's trailing edge. In *Tiktaalik*, rays show a similar pattern; they reach to the base of the radius anteriorly and become more distal posteriorly. Although postaxial rays are not preserved in close association with endoskeletal elements in *Tiktaalik*, these rays would likely have been positioned distal to the ulnare and associated with the radials posterior to the third and fourth mesomeres. The pattern of preaxial rays being more proximal is likely plesiomorphic to sarcopterygians (45, 46), although it can vary [e.g., an inverse pattern in *Neoceratodus* (Fig. 4) and a symmetrical pattern in *Glyptolepis* (46) and *Latimeria* (47)].

The pectoral fin rays of tetrapodomorphs are patterned along the anteroposterior axis. Uniformly, anterior rays are more robust, and species differ in the degree and spatial patterns of heterogeneity. For example, in *Sauripterus*, rays vary in thickness and in the geometry of hemitrichia proximally (Fig. 1*A*). In *Eusthenopteron*, the anterior rays are nonbranching and slightly thicker than more posterior rays (Fig. 2 *A* and *B*). In *Tiktaalik*, the majority of the rays (anterior two-thirds) are unsegmented and nonbranching, and anterior rays are thicker than posterior rays (*SI Appendix*, Fig. S5). Among tetrapodomorphs, only the proposed elpistostegid *Howittichthys* (28) has been described similarly, with anterior rays of the pectoral fin that are unsegmented and unbranching (28).

The tetrapodomorph pectoral fin web was plesiomorphically of equal or greater size than the lobed region. This is observed in both *Sauripterus* and *Eusthenopteron* (Figs. 1 and 2) and in many other species [e.g., *Osteolepis* (Osteolepidae) (48), *Gooloogongia* (Rhizodontida) (31), *Cladarosymblema* (Megalichthyidae) (31), and *Panderichthys* (Elpistostegalia) (49)]. Only 2 tetrapodomorph taxa deviate from this pattern: *Tiktaalik* and *Howittichthys* (28). In both cases, the fin web is substantially smaller than the lobed component of the fin. It is unlikely that the reduced lepidotrichia length in these species is due to distal breakage. *Tiktaalik* rays are of consistent length at the distal tip in specimens NUFV109 and NUFV110, and in both species, specimens are preserved with a posterior distal fringe, where fragile and segmented components of the rays are preserved, although disarticulated (*SI Appendix*, Fig. S5) (28).

Given the crownward phylogenetic position of *Tiktaalik*, we predict that dermal fin rays of pectoral fins become consolidated, reducing segmentation and branching, and that the length of the fin web was reduced prior to the fin-to-limb transition. Given the limited materials preserved of *Howittichthys*, it is difficult to confidently assign its phylogenetic position (28) and to determine whether similarities with *Tiktaalik* in pectoral fin ray morphology reflect homoplasy or a plesiomorphic pattern among crownward elpistostegids.

The pectoral fin rays of *Tiktaalik* have converged on morphologies observed in benthic actinopterygians. Ray-finned fishes have repeatedly evolved to occupy benthic niches (50). In these lineages, the fin web often becomes regionalized, and lepidotrichia that are in frequent contact with the substrate become unbranched, shorter, and thicker (50–55). These morphological changes correlate with functional changes, specifically increased flexural stiffness (i.e., resistance to bending) of fin rays (56). The consolidated rays and reduced fin length in *Tiktaalik* are, therefore, consistent with previous predictions that its paired fins were adapted for interaction with the substrate (12) and suggest selection for a stiffened fin web.

Asymmetry in Hemitrichial Coverage. The pectoral fins of sarcopterygians exhibit asymmetry in the extent to which dorsal and ventral rays cover the endoskeleton. This pattern is observed in *Neoceratodus*, *Eusthenopteron*, and *Tiktaalik*. Species differ in the region of the fin that this asymmetry occurs and in the degree of this asymmetry. Asymmetries in the distribution of hemitrichia have implications for the distribution of fin ray musculature. In gnathostomes, pectoral fins plesiomorphically had dorsal and ventral muscles (i.e., fin ray extensors and flexors, respectively) that originate from the pectoral girdle and insert on the bases of the dermal rays (5). This is seen in *Latimeria*, for example, where muscles attach distally to an aponeurotic fascia that spans the proximal tips of the dermal rays (47, 57). Thus, dorsoventral asymmetry in the proximal extent of hemitrichia should correlate with the distal extent of fin ray extensors and flexors. In *Eusthenopteron*, pectoral fin flexors are predicted to have extended slightly more distally than extensors on the preaxial side. Similarly, in *Tiktaalik*, the ventral surface of the fin would have been significantly more muscular than the dorsal surface distally. Flexors would have covered the ventral surfaces of the third and fourth mesomeres, analogous to a muscular "palm," a pattern that had not been documented previously in tetrapodomorph fins.

Geological and anatomical evidence is strongly indicative that *Tiktaalik* was an animal interacting with the substrate in an aquatic context (12, 42, 43). However, changes in the distribution of paired fin musculature would have had implications for terrestriality in future tetrapodomorphs. Dorsal extensor muscles, which were adapted for fin protraction and resisting hydrodynamic drag, would become adapted to limb protraction during the swing phase of walking. Additionally, ventral flexor muscles, which were adapted for propulsion, stability, and supporting weight underwater, would become adapted for elevating the body on land. The dorsoventral asymmetry of distal fin musculature was an important precursor to the architecture of limbs, foreshadowing the anatomical and functional differences between the flexors and extensors of digits in terrestrial tetrapods.

In sarcopterygians, fin rays can span endoskeletal joints (Figs. 1, 3, and 4). This is predicted to restrict movement at the articular surfaces of the endoskeleton and stiffen the fin lobe (20). This functional relation between dermal rays and the endoskeleton is distinct from that of teleost paired fins, where distal radials act as pivot points on which hemitrichia flex and extend to precisely modulate the stiffness, curvature, and area of the fin web (58, 59). In *Tiktaalik*, the dorsal hemitrichia span the joints of the third, fourth, and fifth mesomeres. Likely, this would have limited extension and flexion of these joints, consolidating the distal endoskeletal elements into a functional unit. Previous analysis of the pectoral fin endoskeleton and girdle of *Tiktaalik* predicted that the animal was capable of propping its body off of the substrate, achieving an elevated, fin-supported stance through flexure of the shoulder and elbow and extension of the endoskeleton distal to the ulnare and intermedium (12). Notably, the distal domain predicted to have been in flexion during an elevated stance corresponds to the domain that we diagnose here as functionally integrated by dorsal hemitrichial coverage. This domain also lacks ventral rays. If scales were also absent this palmar region, it is possible that ventral rays were lost to minimize damage, either by abrasion or breakage, that would have been incurred upon loading of the fin against the substrate.

Asymmetry in Hemitrichia Morphology. The dorsal and ventral hemitrichia of tetrapodomorph pectoral fins differ in their CSA (Fig. 5). To our knowledge, asymmetries in the CSA of dorsal and ventral rays have not been described previously but seem to characterize the paired fins of crown group osteichthyans (*SI Appendix*, Fig. S7). The degree of asymmetry in CSA is modest in *Eusthenopteron* and consistent between specimens differing nearly 4-fold in size. By contrast, *Tiktaalik* exhibits high-magnitude differences in CSA, and the degree of difference is greater in the larger individual.

It is difficult to rigorously determine phylogenetic patterns in tetrapodomorphs because data of this type are currently available only for 2 tetrapodomorph species. However, the dermal rays of *Eusthenopteron* appear to broadly reflect the general tetrapodomorph condition (e.g., anteroposterior ray distribution, segmentation and branching patterns, length, slight asymmetry in dorsoventral coverage). Thus, a slight asymmetry with larger dorsal rays is inferred to be the plesiomorphic tetrapod condition, and a high magnitude of asymmetry, as in *Tiktaalik*, is inferred to be a derived condition among crownward tetrapodomorphs. Additionally, despite a limited number of individuals (2 per species), comparisons of specimens of different sizes allow for hypotheses of growth trajectory. We predict that the dorsal and ventral hemitrichia of *Eusthenopteron* scaled isometrically (the ratio of CSAs being consistent across size classes), whereas those of *Tiktaalik* scaled allometrically (the ratio of CSAs changing as the animal grew, with hemitrichia becoming more asymmetric at larger sizes).

The functional implications of asymmetry in hemitrichial size and shape are unclear. Isometric scaling of hemitrichia in *Eusthenopteron* would suggest that pectoral fin function is consistent across postlarval sizes. This is supported by previous work demonstrating that pectoral fin position is consistent for a wide range of standard lengths (35). Allometric scaling of the hemitrichia of *Tiktaalik* would indicate that pectoral fin mechanics and loading regimes change as the animal grows. Given that other features of *Tiktaalik* fin rays, described above, appear to correspond with increasing stiffness, we propose that these asymmetries, by locally increasing CSA, increase flexural stiffness

(*SI Appendix*, Fig. S8) (56) and provide resistance to buckling in dorsal rays when loaded from the ventral side. Testing this hypothesis will require analyzing the functional morphology of modern analogs and expanding in silico models of hemitrichial mechanics (58) into asymmetric morphospaces. The evolution of dorsoventral asymmetries in dermal fin rays is likely an important axis of diversification in fish fins. The observation of asymmetries in a variety of osteichtyans lineages indicates that this property is relevant to fin design broadly, not only for substrate-associated fins. For example, fins used for rowing might have dorsoventrally asymmetric hemitrichia if kinematics and hydrodynamic loading regimes differ between fore and aft strokes.

We predict that, during embryonic development, asymmetries can develop by the differential expression of signaling or transcription factor genes between the dorsal and ventral epithelium of the larval fin fold. These dermal skeletal asymmetries and also, more proximal asymmetries in the paired fins [e.g., endochondral articular surfaces, distribution of musculature, and ventral vasculature grooves (*SI Appendix*, 3-dimensional image)] are likely patterned by Wnt signaling pathways, similar to developing limbs (60, 61). Postembryonic growth patterns observed in *Tiktaalik* also raise the intriguing possibility of a plastic response by dermal rays to mechanical loading and that such plasticity contributed to the evolution of substrate-associated behaviors in tetrapodomorphs, similar to what has been hypothesized for the girdle (62) and gill arches in response to aerial environments (63, 64). It is currently unknown whether fin rays can respond in a plastic manner to loading of the fin web.

Tetrapodomorph paired fins were plesiomorphically adapted to resist hydrodynamic loads. In the lineage leading to crown group tetrapods, paired appendages became adapted to substrate-based loading and supporting the weight of the animal. Understanding how this transition in function occurred requires consideration of all parts of the paired fins, not simply the endoskeleton. This study shows that that, prior to the fin-to-limb transition, fin rays had evolved morphologies convergent to benthic actinopterygians (consolidated fin rays and a reduced fin web). Additionally, the evolution of increased asymmetry between dorsal and ventral hemitrichia provides clarity as to how an elevated, fin-supported posture was achieved in *Tiktaalik*. Selection on fin ray morphology in response to a benthic lifestyle might have been an important transitionary step prior to the origin of digits and extended incursions by tetrapods into terrestrial ecosystems.

Methods

CT Scanning. Scans of *Sauripterus*, *Eusthenopteron*, *Tiktaalik*, and *Polypterus* were collected at The University of Chicago's PaleoCT scanning facility using a GE Phoenix v|tome|x 240 kv/180 kv scanner (http://luo-lab.uchicago.edu/paleoCT.html). CT data were reconstructed with Phoenix Datos|x 2 (version 2.3.3) and imported to VGStudio Max (version 2.2) to be cropped and exported as a tiff stack. *Neoceratodus* and *Acipenser* were scanned at the Harvard University Center for Nanoscale Systems with the HMXST Micro-CT X-ray imaging system (model HMXST225). Scan settings are presented in *SI Appendix*, Table S1. CT data were segmented and visualized in Amira 6.5 (FEI Software). Movies were generated by first exporting animations as tiff stacks from Amira and then combining and editing movies using Adobe Premier (version 13.12).

Quantifying Hemitrichial Asymmetry. For each specimen analyzed, we selected a set of 3 adjacent lepidotrichia that were straight and unbroken. Individual hemitrichia were segmented using Amira and exported as 2-dimensional tiff stacks. These data were then imported to Fiji (version 2.0.0-cr-69/1.52n) (65) as "Raw Sequences" and converted to binary using the Huang method. Specimens were scaled by setting pixel size to the voxel dimensions from the CT scan. Using the package BoneJ (version 1.4.3) (66), we applied the "Moments of Inertia" function using default settings for all slices. This resulted in an image stack with orientation that corresponded to the long axis of the ray. Next, we applied the function "Slice Geometry" on the aligned data to recover CSAs and SMAs of slices orthogonal to the long axis of the ray. Finally, we trimmed the terminal few cross-sections, which are artificially small due to the fact that rays were not clipped precisely orthogonal to their long axis during extraction in Amira.

We compared the CSA and SMA of the dorsal and ventral hemitrichia of each lepidotrichium. A Shapiro test was used to assess whether the distributions of CSA and SMA were normal. Tests generally recovered P values < 0.05, implying that the distribution of the data is significantly different from normal. Therefore, we next conducted Mann–Whitney U test, which allows testing of whether population distributions are identical without assuming them to be normal. All statistical analyses were performed using R (version 3.3.1). Data were plotted using ggplot2 (version 3.1.0) (67).

When comparing SMA, we analyzed SMAs around neutral axes that corresponded with the pectoral fin's dorsoventral axis (*SI Appendix*, Fig. S8). For most hemitrichia, this inference is straightforward, with rays displaying distinct morphological polarity and reliable orientation within the fin web. However, the ventral hemitrichia of *Tiktaalik* pectoral fins do not show clear anatomical markers, and it is possible that they were displaced or rotated during preservation (e.g., Fig. 3*D* shows ventral rays slightly displaced and oblique to the dorsal rays). Therefore, to assess whether the results described are robust to alternative ventral ray orientations, we also considered alternative neutral axis of bending: the SMA around the minor axis. Results presented above are consistent between the different axes of bending: the magnitude of asymmetry in SMA is greater in *Tiktaalik* than other species, and it is greater in the larger *Tiktaalik* individual.

Data Availability. μCT data for *Sauripterus* (ANSP20581), *Eusthenopteron* (CMNH 10926, CMNH 8153), *Tiktaalik* (NUFV109, NUFV110), *Neoceratodus* (MCZ157440), *Polypterus* (FMNH1217440), and *Acipenser* (FMNH144017) are available on MorphoSource (Project P853) (68). Three-dimensional surface models of the endoskeletal and dermal skeletal elements of *Tiktaalik* (NUFV110) and *Sauripterus* (ANSP20581) pectoral fins are also available in the project. CSA and SMA values of each hemitrichia analyzed are available on the Dryad Digital Repository (https://doi.org/10.5061/dryad.2fqz612kd) (69). The R code for analysis and plotting is available on GitHub (https://github.com/ThomasAStewart/tetrapodomorph_dermal_project) (70).

ACKNOWLEDGMENTS. We thank A. McGee at the Cleveland Museum of Natural History for access to *Eusthenopteron* specimens and C. McMahan, S. Mochel, and K. Swagel at the Field Museum of Natural History for access to actinopterygian specimens. We thank N. Loughlin for her work on *Neoceratodus* and sturgeon reconstructions. *Tiktaalik* specimens were prepared by Frederick Mullison and Robert Masek. William Downs and Frederick Mullison prepared the specimens of *Sauripterus*. We also thank M. I. Coates and G. V. Lauder for comments on the material. Financial support came from The Brinson Foundation, an anonymous donor to the Academy of Natural Sciences, the Biological Sciences Division of The University of Chicago, and the NSF (E.B.D. and N.H.S.). This material is based on work supported by NSF Grants EAR 0207721 (to E.B.D.), EAR 0544093 (to E.B.D.), EAR 0208377 (to N.H.S.), and EAR 0544565 (to N.H.S.).

1. M. I. Coates, The origin of vertebrate limbs. *Dev. Suppl.* **1994**, 169–180 (1994).
2. P. Janvier, *Early Vertebrates* (Oxford Monographs on Geology and Geophysics, Clarendon Press, Oxford, United Kingdom, 1996), vol. 33.
3. J. A. Clack, *Gaining Ground: The Origin and Evolution of Tetrapods* (Indiana University Press, ed. 2, 2012).
4. R. Owen, *On the Nature of Limbs* (John Van Voorst, London, United Kingdom, 1849).
5. E. S. Goodrich, *Studies on the Structure and Development of Vertebrates* (Macmillan, London, United Kingdom, 1930).
6. A. Romer, F. Byrne, The pes of *diadectes*: Notes on the primitive tetrapod limb. *Paleobiologica* **4**, 25–48 (1931).
7. N. Holmgren, On the origin of the tetrapod limb. *Acta Zool.* **14**, 185–295 (1933).
8. W. Gregory, H. Raven, Origin of paired fins and limbs. *Ann. N. Y. Acad. Sci.* **42**, 273–360 (1941).
9. N. H. Shubin, P. Alberch, A morphogenetic approach to the origin and basic organization of the tetrapod skeleton. *Evol. Biol.* **20**, 319–387 (1986).
10. M. Coates, J. Clack, Polydactyly in the earliest known tetrapod limbs. *Nature* **347**, 66–69 (1990).
11. G. P. Wagner, C.-H. Chiu, The tetrapod limb: A hypothesis on its origin. *J. Exp. Zool.* **291**, 226–240 (2001).
12. N. H. Shubin, E. B. Daeschler, F. A. Jenkins Jr, The pectoral fin of *Tiktaalik roseae* and the origin of the tetrapod limb. *Nature* **440**, 764–771 (2006).
13. B. K. Hall, *Fins into Limbs: Evolution, Development and Transformation* (University of Chicago Press, Chicago, IL, 2007).

14. J. A. Clack, The fin to limb transition: New data, interpretations, and hypotheses from paleontology and developmental biology. *Annu. Rev. Earth Planet. Sci.* **37**, 163–179 (2009).
15. C. A. Boisvert, E. Mark-Kurik, P. E. Ahlberg, The pectoral fin of *Panderichthys* and the origin of digits. *Nature* **456**, 636–638 (2008).
16. K. Onimaru *et al*., A shift in anterior-posterior positional information underlies the fin-to-limb evolution. *eLife* **4**, e07048 (2015).
17. K. Onimaru, L. Marcon, M. Musy, M. Tanaka, J. Sharpe, The fin-to-limb transition as the re-organization of a Turing pattern. *Nat. Commun.* **7**, 11582 (2016).
18. T. A. Stewart, R. Bhat, S. A. Newman, The evolutionary origin of digit patterning. *Evodevo* **8**, 21 (2017).
19. K. S. Thomson, New evidence on the evolution of the paired fins of Rhipidistia and the origin of the tetrapod limb, with description of a new genus of Osteolepididae. *Postilla* **157**, 1–7 (1972).
20. M. C. Davis, N. Shubin, E. B. Daeschler, A new specimen of *Sauripterus taylori* (Sarcopterygii, Osteichthyes) from the Famennian Catskill Formation of North America. *J. Vertebr. Paleontol.* **24**, 26–40 (2004).
21. J. E. Jeffery, G. W. Storrs, T. Holland, C. J. Tabin, P. E. Ahlberg, Unique pelvic fin in a tetrapod-like fossil fish, and the evolution of limb patterning. *Proc. Natl. Acad. Sci. U.S.A.* **115**, 12005–12010 (2018).
22. W. Harder, *Anatomy of Fishes* (Schweizerbart Science Publishers, Stuttgart, Germany, 1976).
23. R. Freitas, C. Gómez-Marín, J. M. Wilson, F. Casares, J. L. Gómez-Skarmeta, Hoxd13 contribution to the evolution of vertebrate appendages. *Dev. Cell* **23**, 1219–1229 (2012).
24. T. Nakamura, A. R. Gehrke, J. Lemberg, J. Szymaszek, N. H. Shubin, Digits and fin rays share common developmental histories. *Nature* **537**, 225–228 (2016).
25. E. S. Goodrich, Memoirs: On the dermal fin-rays of fishes—living and extinct. *Q. J. Microsc. Sci.* **47**, 465–522 (1904).
26. E. Jarvik, Dermal *Fin-Rays* and Holmgren's Principle of *Delamination* (Kungl. Svenska vetenskapsakademiens handlingar, Almqvist & Wiksell, Stockholm, Sweden, 1959), p. 51.
27. S. M. Andrews, T. S. Westoll, IX.—The postcranial skeleton of *Ensthenopteron foordi* Whiteaves. *Trans. R. Soc. Edinb.* **68**, 207–329 (1970).
28. J. A. Long, T. Holland, A possible elpistostegalid from the Devonian of Gondwana. *Proc. R. Soc. Vic.* **120**, 182–192 (2008).
29. S. M. Andrews, Rhizodont crossopterygian fish from the Dinantian of Foulden, Berwickshire, Scotland, with a re-evaluation of this group. *Trans. R. Soc. Edinb. Earth Sci.* **76**, 67–95 (1985).
30. Z. Johanson, P. E. Ahlberg, Devonian rhizodontids and tristichopterids (Sarcopterygii; Tetrapodomorpha) from East Gondwana. *Trans. R. Soc. Edinb. Earth Sci.* **92**, 43–74 (2001).
31. T. Holland, Pectoral girdle and fin anatomy of *Gogonasus andrewsae* long, 1985: Implications for tetrapodomorph limb evolution. *J. Morphol.* **274**, 147–164 (2013).
32. J. Rackoff, *The Terrestrial Environment and the Origin of Land Vertebrates*, A. L. Panchen, Ed. (Systematics Association, London, United Kingdom, 1980), p. 633.
33. M. C. Davis, N. Shubin, E. B. Daeschler, Immature rhizodontids from the Devonian of North America. *Bull. Mus. Comp. Zool.* **156**, 171–187 (2001).
34. J. Hall, *Natural History of New York. Part IV. Geology Comprising the Survey of the Fourth Geological District* (D. Appleton & Company, New York, NY, 1842), p. 683.
35. H.-P. Schultze, Juvenile specimens of *Eusthenopteron foordi* Whiteaves, 1881 (osteolepiform rhipidistian, Pisces) from the Late Devonian of Miguasha, Quebec, Canada. *J. Vertebr. Paleontol.* **4**, 1–16 (1984).
36. K. S. Thomson, K. V. Hahn, Growth and form in fossil rhipidistian fishes (Crossopterygii). *J. Zool.* **156**, 199–223 (1968).
37. S. Cote, R. Carroll, R. Cloutier, L. Bar-Sagi, Vertebral development in the Devonian Sarcopterygian fish *Eusthenopteron foordi* and the polarity of vertebral evolution in non-amniote tetrapods. *J. Vertebr. Paleontol.* **22**, 487–502 (2002).
38. M. Laurin, F. J. Meunier, D. Germain, M. Lemoine, A microanatomical and histological study of the paired fin skeleton of the devonian sarcopterygian *Eusthenopteron foordi*. *J. Paleontol.* **81**, 143–153 (2007).
39. T. Holland, J. A. Long, On the phylogenetic position of *Gogonasus andrewsae* Long 1985, within the Tetrapodomorpha. *Acta Zool.* **90**, 285–296 (2009).
40. J. E. Jeffery, Cranial morphology of the Carboniferous rhizodontid *Screbinodus ornatus* (Osteichthyes: Sarcopterygii). *J. Syst. Palaeontology* **10**, 475–519 (2012).
41. J. Lu *et al*., The earliest known stem-tetrapod from the Lower Devonian of China. *Nat. Commun.* **3**, 1160 (2012).
42. E. B. Daeschler, N. H. Shubin, F. A. Jenkins Jr, A Devonian tetrapod-like fish and the evolution of the tetrapod body plan. *Nature* **440**, 757–763 (2006).
43. N. H. Shubin, E. B. Daeschler, F. A. Jenkins Jr, Pelvic girdle and fin of *Tiktaalik roseae*. *Proc. Natl. Acad. Sci. U.S.A.* **111**, 893–899 (2014).
44. E. Jarvik, *Basic Structure and Evolution of Vertebrates* (Academic, New York, NY, 1980), vol. 1.
45. E. Jude, Z. Johanson, A. Kearsley, M. Friedman, Early evolution of the lungfish pectoral-fin endoskeleton: Evidence from the middle devonian (Givetian) *Pentlandia macroptera*. *Front. Earth Sci.* **2**, 10.3389/feart.2014.00018 (2014).
46. P. E. Ahlberg, Paired fin skeletons and relationships of the fossil group Porolepiformes (Osteichthyes: Sarcopterygii). *Zool. J. Linn. Soc.* **96**, 119–166 (1989).
47. P. J. Millot, J. Anthony, *Anatomie de Latimeria chalumnae: Tome 1: Squelette, Muscles et Formations de soutien* (Éditions du Centre National de la Recherche Scientifique, Paris, France, 1958).
48. E. Jarvik, *On the Morphology and Taxonomy of the Middle Devonian Osteolepid Fishes of Scotland* (Almqvist & Wiksells boktr., 1948).
49. E. Vorobyeva, H.-P. Schultze, *Origins of the Higher Groups of Tetrapods: Controversy and Consensus*, H.-P. Schultze, L. Trueb, Eds. (Cornell Univ. Press, Ithaca, NY, 1991), pp. 68–109.
50. J. G. Lundberg, E. Marsh, Evolution and functional anatomy of the pectoral fin rays in cyprinoid fishes, with emphasis on the suckers (family Catostomidae). *Am. Midl. Nat.* **96**, 332–349 (1976).
51. E. Marsh, Structural modifications of the pectoral fin rays in the order Pleuronectiformes. *Copeia* **1977**, 575–578 (1977).
52. R. Brandstätter, B. Misof, C. Pazmandi, G. P. Wagner, Micro-anatomy of the pectoral fin in blennies (Blenniini, Blennioidea, Teleostei). *J. Fish Biol.* **37**, 729–743 (1990).
53. N. K. Taft *et al*., Comparative morphology and mechanical properties of the lepidotrichia of climbing and non-climbing Hawaiian gobioid fishes. *Cybium* **41**, 107–115 (2017).
54. N. K. Taft, G. V. Lauder, P. G. A. Madden, Functional regionalization of the pectoral fin of the benthic longhorn sculpin during station holding and swimming. *J. Zool.* **276**, 159–167 (2008).
55. N. K. Taft, B. N. Taft, Functional implications of morphological specializations among the pectoral fin rays of the benthic longhorn sculpin. *J. Exp. Biol.* **215**, 2703–2710 (2012).
56. B. R. Aiello *et al*., A comparison of pectoral fin ray morphology and its impact on fin ray flexural stiffness in labriform swimmers. *J. Morphol.* **279**, 1031–1044 (2018).
57. T. Miyake *et al*., The pectoral fin muscles of the coelacanth *Latimeria chalumnae*: Functional and evolutionary implications for the fin-to-limb transition and subsequent evolution of tetrapods. *Anat. Rec. (Hoboken)* **299**, 1203–1223 (2016).
58. S. Alben, P. G. Madden, G. V. Lauder, The mechanics of active fin-shape control in ray-finned fishes. *J. R. Soc. Interface* **4**, 243–256 (2007).
59. M. I. Coates, K. Tietjen, 'This strange little palaeoniscid': A new early actinopterygian genus, and commentary on pectoral fin conditions and function. *Earth Environ. Sci. Trans. R. Soc. Edinburgh* **109**, 15–31 (2019).
60. R. D. Riddle *et al*., Induction of the LIM homeobox gene Lmx1 by WNT7a establishes dorsoventral pattern in the vertebrate limb. *Cell* **83**, 631–640 (1995).
61. M. Kengaku *et al*., Distinct WNT pathways regulating AER formation and dorsoventral polarity in the chick limb bud. *Science* **280**, 1274–1277 (1998).
62. E. M. Standen, T. Y. Du, H. C. Larsson, Developmental plasticity and the origin of tetrapods. *Nature* **513**, 54–58 (2014).
63. A. J. Turko *et al*., Skeletal stiffening in an amphibious fish out of water is a response to increased body weight. *J. Exp. Biol.* **220**, 3621–3631 (2017).
64. P. A. Wright, A. J. Turko, Amphibious fishes: Evolution and phenotypic plasticity. *J. Exp. Biol.* **219**, 2245–2259 (2016).
65. J. Schindelin *et al*., Fiji: An open-source platform for biological-image analysis. *Nat. Methods* **9**, 676–682 (2012).
66. M. Doube *et al*., BoneJ: Free and extensible bone image analysis in ImageJ. *Bone* **47**, 1076–1079 (2010).
67. H. Wickham, *ggplot2: Elegant Graphics for Data Analysis* (Springer-Verlag, New York, NY, 2016).
68. T. A. Stewart *et al*., Project: Fin ray patterns at the fin to limb transition. MorphoSource. https://www.morphosource.org/Detail/ProjectDetail/Show/project_id/853. Deposited 15 December 2019.
69. T. A. Stewart *et al*., Data from: Fin ray patterns at the fin to limb transition. Dryad. https://datadryad.org/stash/dataset/doi:10.5061/dryad.2fqz612kd. Deposited 16 December 2019.
70. T. A. Stewart, Tetrapodomorph Dermal Project. GitHub. https://github.com/ThomasAStewart/tetrapodomorph_dermal_project/. Deposited 15 December 2019.